Brine seepage tracing in a damaged dam slope using elapsed-time electrical resistivity tomography

Helsin Wang[1], Keng-Tsang Hsu[2], Chih-Hsin Hu[1], Chih-Hsien Hsieh[3], Ying-Tzu Ke[2*]

[1] *HCK Geophysical, Roosevelt Road, Taipei 106012, Taiwan*
[2] *Department of Civil and Construction Engineering, Chaoyang University of Technology, Wufeng District, Taichung, 413310, Taiwan*
[3] *Sinotech Construction Corporation, Ltd., Nanking East Road, Taipei 105409, Taiwan*

ABSTRACT

The electrical resistivity tomography technique is a geophysical inspection method widely used for several investigations, such as mining exploration, fault localization, groundwater flow, geological exploration, and pollution zones. Infusing brine into substructure can increase conductivity and becomes a useful medium to trace the path of the seepage flowing in rockfill dams. In this article, an elapsed-time electrical resistivity tomography technique was developed to monitor the potential seepage in the damaged dam slopes nearby a concrete spillway. Tracing the downhole brine seepage could effectively identify the possible direction and path of the seepage flowing through the rockfill dam mass in a few hours. The spatial distribution variations of electrical resistivity tomography images can also provide information about the potential sliding surface and the accumulation zones of the seepage in the downstream side slope of the dam.

Keywords: Electrical resistivity tomography, Brine seepage tracing, Elapsed-time, Slope failure, Groundwater, Dam.

OPEN ACCESS

1. INTRODUCTION

Permeability of rocks and soils, features of geological structures, groundwater conditions, or underground anomalies, including mining pits and sinkholes, could directly influence the seepage conditions around a dam site or its watershed (Hung, 2016). In general, sandstone, mudstone, or limestone have a relatively higher permeability than that of shale or granite. Fractured rocks nearby faults or fault belts, or rocks with tension cracks adjacent anticline crests could feasibly lead to the leakage at dam foundations. Besides, a bedding plane dipping to the downstream side could also have a higher possibility to form a groundwater channel on rockfill or earth dam sites.

The most crucial investigation is to determine the watertightness conditions around dam sites for reservoir planning and construction. The survey items of watertightness usually consist of groundwater table, groundwater pressure, permeability/conductivity in soils or rocks, geological investigation, and borehole exploration (Hung, 2016).

Electrical resistivity tomography, one of the near-surface geophysical inspection techniques, has been applied to the investigation on groundwater flow or seepage for several years (Schuster and Krizek, 1978; Wightman et al., 2003; TGS, 2011; Tesfaldet and Puttiwongrak, 2019). In this article, an elapsed-time electrical resistivity tomography inspection was introduced to monitor the seepage trend of groundwater nearby the damaged spillway slope of a rockfill dam by tracing the infused brine flow.

2. DESCRIPTION OF ELECTRICAL RESISTIVITY TOMOGRAPHY

2.1 Background

The resistivity method is a non-destructive approach used for subsurface condition investigation. Conrad Schlumberger first performed the electrical resistivity field surveys in the beginning of the 20th century (Ward, 1980). Ever since, the method has been developing in the ascendant, and new application areas have moved forward. During the past few decades, this development has been particularly rapid, considering the introduction of innovative efficient instruments and the fast progress of easily available computational power (Sjödahl, 2006).

The electrical resistivity tomography method has been used for a wide range of near-surface geological, engineering, and environmental purposes (Ward, 1990; Wightman et al., 2003; Daily et al., 2005; Sjödahl, 2006; Society of Exploration Geophysicists of Japan, 2014). The electrical resistivity tomography inspection technique can identify or localize geological layers, faults, groundwater pollutants, cavities, mining strata, burial layers, or landslide mass, as well as for various practical applications. For example, using this survey method can explore construction materials, such as sand and gravel within the mining industry, support site investigations and geotechnical applications for all types of civil engineering projects, and map soil/bedrock interfaces, groundwater levels, faults, and crosszones in geological prospecting field. The applications of the electrical resistivity tomography inspection technique cover several areas, such as monitoring of potential landslides, contamination and integrity in landfills, leakage or seepage monitoring in embankment dams or barriers, salt-water intrusion in coastal areas, pollution investigations or control in mining sites, exploration and protection of groundwater resources, geothermal investigation in energy industry, or archaeological delineation (e.g., Ward, 1990; Dahlin, 1993; Pellerin, 2002).

For the specific purposes in seepage through rock/soil mass, the capability of this inspection technique can effectively identify the interfaces between weathering zone and bedrock, and field survey for fault zone/ shear zone, fracture zone, colluvium, or sliding plane (Liao et al., 2019). The site selection for embankment dams also needs the in-situ watertightness information by using electrical resistivity tomography inspection technique (Hung, 2016). One can use the electrical resistivity tomography inspection technique for the watershed survey on groundwater recharge condition affecting by seasonal factors (Tesfaldet and Puttiwongrak, 2019), post-disaster forensic investigation (Schuster and Krizek, 1978; Wightman et al., 2003; TGS, 2011), or more detailed geological substructral information with borehole high-resolution electrical resistivity tomography images (Lin et al., 2019), as well.

2.2 Principle and Application

The principle of electrical resistivity tomography is to develop an artificial potential field by probing one pair of current electrodes, labelled as A and B, into the ground around a target zone, as shown in Fig. 1. Two extra electrodes, labelled as M and N, are used to measure the ground resulting potential difference. The most common resistivity systems use direct current, DC, or alternating currents, AC, with very low frequency. Some electrical resistivity tomography techniques use line electrodes or buried electrodes, but the most commonly-used method involves point electrodes on the surface. Typically one pair of steel electrodes is used to inject current and another pair is used to measure the potentials. This type of four-electrode measurement avoids erroneous external influence on measurements from contact resistance at the interface between the electrode and the ground (Sjödahl, 2006).
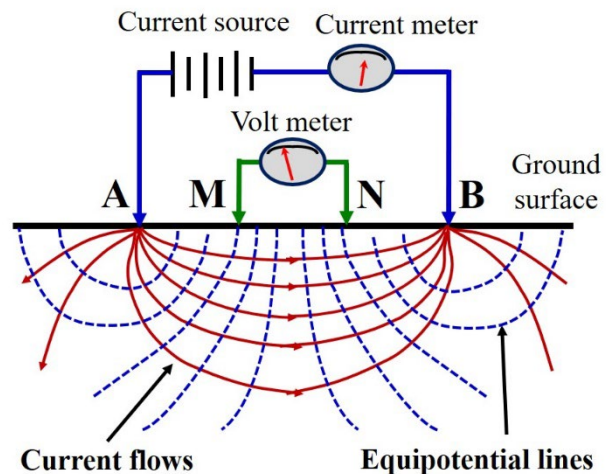

Fig. 1. Electrical resistivity tomography inspection schametic

A typical apparent resistivity image is usually displayed with a visible-light mode, which corresponds to the resistivity values varying from 2,000 to less than 1 $\Omega \times$ m, as shown in Fig. 2. The typical resistivity values for sediments composed of boulder, gravel, and sand are more than 60 $\Omega \times$ m, corresponding to the pink, red, orange, yellow, or green zones. Water, pollutant, or metal represents low resistivity zones, corresponding to the blue and light blue shades. A significant low-resistivity closed-contour zone is usually located right below the bridge pier, and the bottom of this low-resistivity zone, marked with a dashed-lined rectangle, can be identified as the depth of the bridge foundation, which usually consists of conductive reinforced steel rebars. The locations and depths of any possible subsurface anomalies can be effectively identified with this two-dimensional resistivity image profiles. In addition, the most commonly-useful array configurations are pole-dipole and dipole-dipole methods for foundation inspection (Wang et al., 2015).
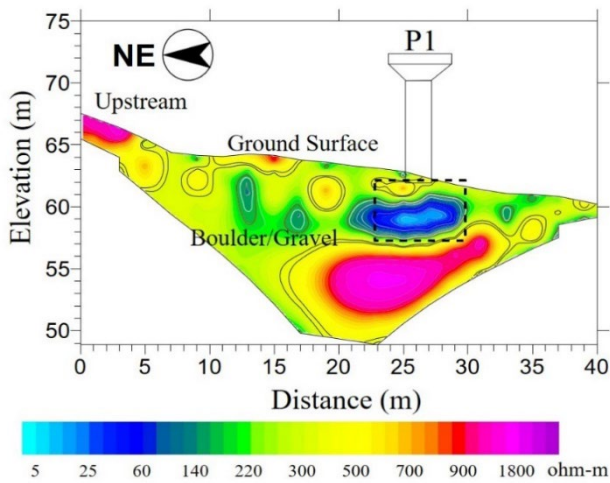
Fig. 2. Electrical resistivity tomography inspection on an unknown bridge foundation

Table 1. Resistivity range of common rocks, soils, and water (after Loke, 2000)

Material	Resistivity (ohm × m)
Rock	
Granite	$5 \times 10^3 - 10^6$
Slate	$6 \times 10^2 - 4 \times 10^7$
Marble	$10^2 - 2.5 \times 10^8$
Sandstone	$8 - 4 \times 10^3$
Shale	$20 - 2 \times 10^3$
Limestone	$50 - 4 \times 10^2$
Soil	
Clay	$5 \times 10^3 - 2 \times 10^4$
Sand (dry)	$2 \times 10^2 - 10^3$
Sand (saturated)	$2 \times 10^4 - 8 \times 10^4$
Gravel (dry)	$1 - 100$
Gravel (saturated)	$10^3 - 5 \times 10^3$
Alluvium	$10 - 800$
Water	
Groundwater (fresh)	$10 - 100$
Sea Water	0.2

The on-site resistivity values are also highly associated with mineral composition, grain size, mineral formation, water content, and ion concentration (Loke, 2000; Society of Exploration Geophysicists of Japan, 2014). Table 1 shows typical resistivity value ranges for geomaterials and water. Generally, rocks have relatively higher resistivity values. Soils have a broader and lower resistivity ranges highly related to their water content. Seawater, containing more ions, has lower resistivity values than those of both soils and rocks. This feature implies that brine, fresh water mixing with salt particles, could be a useful medium to trace the path and flowing direction of the groundwater seepage flowing through rockfill or earth dams when using an elapsed-time electrical resistivity tomography technique.

3. SITE CONDITIONS OF THE DAM SLOPE NEARBY A SPILLWAY

The multiple-layered rockfill dam of an off-stream reservoir in southern Taiwan was constructed with selected impervious material core, compact impervious material, riprap cobble, gravel, and sand filter in the 1980s. During the dam construction period, a differential settlement was caused by an undiscovered abandoned river channel on the dam site. The geotechnical engineers found that the non-uniform soft ground could lead to the instability of the entire dam structure. Therefore, the construction contractor decided to launch a ground improvement plan and strengthened the bearing capacity of the dam foundation in order to meet the original design requirements.

An accessory concrete spillway is located at the west side of the minor dam, as shown in Fig. 3. The 1999 Chi-Chi Earthquake in central Taiwan and aftershocks caused several more than 20-m-long vertical cracks along the dam-top paved road of the minor dam. More damage events, like roadside settlement, leakage on the spillway, and lateral movement of the spillway walls, were also found in the post-earthquake safety investigation. An emergency rehabilitation plan, including soil refilling, chemical grouting, curtain grouting, and wall tieback, successfully ceased the detrimental trend and repaired damaged structural components of the spillway (Liming, 2014).
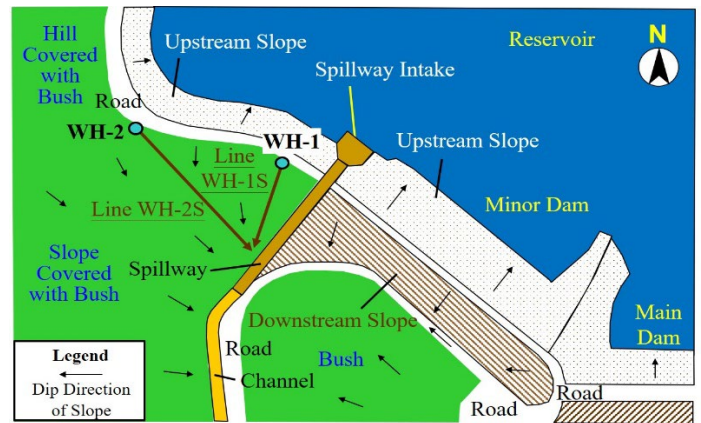

Fig. 3. Top view of the target dams and the spillway (Data from Liming 2014)

In 2013, a typhoon and an accompanying storm triggered the surface sliding of the downstream slope along the spillway again. Leakage and lateral movement were again found on the spillway channel walls (NCTU, 2005; Liming, 2014). Substrate cavitation right below the spillway bottom and piping through the spillway walls directly undermined the stability of the spillway and led to severe cracking on the spillway bottom. Fig. 4 shows the on-site images of the slope failure and damaged spillway channel. The shallow surface sliding removed more than 3.8-m deep topsoils beside the spillway walls. Plastic canvases were covered the

sliding zones to prevent from more surface erosion temporarily. Temporary steel supports were installed along the spillway walls, and substrate refill and retrofitting construction on the channel bottom were conducted for recovering its original function. The post-event report also suggested an in-depth field survey to find the flowing groundwater of the slope failure nearby the spillway (Liming, 2014).

Fig. 4. Surface sliding along the damaged spillway

4. DISCUSSION OF BRINE SEEPAGE TRACING INSPECTION

4.1 Inspection Plan

The electrical resistivity tomography inspection is a well-known technique to spatially inspect the resistivity distribution of geological subsurface. The resistivity responses of soils are usually highly associated with their water content. In this inspection case, considering the overlapping apparent resistivity range between groundwater and soils, brine, i.e., a mixture of water and salt, usually contains more ions and has a much higher conductivity than freshwater. Infusing brine into the subsurface could be a better approach to lower the resistivity values of flowing groundwater temporarily. Therefore, investigators can feasibly identify the seepage conditions of groundwater flowing in the dam mass by using an elapsed-time electrical resistivity tomography technique.

In this paper, a brine seepage tracing technique based on electrical resistivity tomography was applied to know the causes of the piping problem and the surface sliding adjacent the damaged spillway. Two borehole sampling positions, including WH-1 and WH-2, and two electrical resistivity tomography investigation lines were set at the dam-top roadside, as shown in Figs. 3 and 4. A 56-m-long electrical resistivity tomography survey Line WH-1S was extended downward through the sliding slope from borehole WH-1 and measured the subsurface conditions of the sliding mass directly. The dip direction of the geological layers is generally consistent with the slope direction (Liming, 2014). Another 70-m-long electrical resistivity tomography survey Line WH-2S was extended from borehole WH-2 downward along a non-damaged dam slope covered with bush and grass. The electrical resistivity tomography instrument was used to record the background resistivity images before brine infusion. The inspection pattern considered the dipole-diploe survey mode and an electrode spacing of 2 meters.

The concentrations of brine are listed in Table 2 for these two electrical resistivity tomography survey lines. Fig. 5 shows the preparation photos of brine seepage tracing with electrical resistivity tomography technique at two borehole sites. The brine was continuously infused into the dam mass from water tanks at these two boreholes through the PVC pipes. The resistivity variation images were traced at 30, 60, 120, 180, 240 and 840 min after brine injection (Fig. 6). Each inspection period lasted up to 10 min.

4.2 Sliding Zone Investigation

In Fig. 7(a), the geomaterials in the WH-1 borehole sampling, in series, consisted of top soil, weathered sandstone, loose sandstone, loose sandstone with mudstone, and mudstone. The background image of electrical resistivity tomography along survey Line WH-1S, as shown in Fig. 7(b), had a good consistency with the geological findings at borehole WH-1. The black dashed lines represented the geological layer boundaries extended from the borehole sampling with the dip direction of geological layers. The red dotted lines represented the geological layer boundaries jointly defined by both the electrical resistivity tomography image and borehole sampling information. In the background image of electrical resistivity tomography, the top soil and weathering sandstone layers corresponded to relatively low resistivity zones, i.e., light blue and green modes, scattering from the ground surface to depths of 3~5 meters. The yellow, light green, and orange shades, i.e., the relatively high resistivity zones, indicated the sandstone overlaying sandstone with mudstone, i.e., a relatively low resistivity value zone.

Table 2. Mixtures of brine for electrical resistivity tomography tracing

Survey line	Water (m^3)	Salt (kg)	Mixing percentage (%)
WH-1S	1.2	200	16.67
WH-2S	0.6	100	16.67

Fig. 5. Mixing infused brine

Fig. 6. Brine seepage tracing with electrical resistivity tomography technique
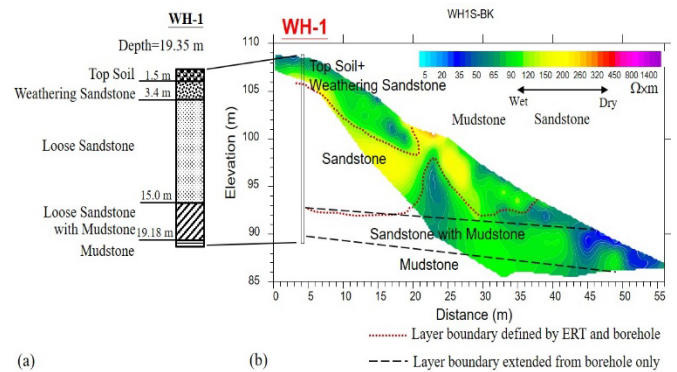

Fig. 7. (a) Geological column at borehole WH-1; (b) background image of electrical resistivity tomography along investigation Line WH-1S (Geological profile data from Liming, 2014)

Fig. 8 represents the resistivity variation images (variation more than -10%) along survey Line WH-1S after infusing brine into borehole WH-1. The resistivity variation images of brine seepage measured the resistivity changes between the background and the influence of brine transmission at a specific moment. Moreover, infusing brine could lead to a significant decrease of the apparent resistivity values in the dam mass when brine flowed through more pervious geological layers. The most intensive resistivity variation zones represented the most intensive influence zones after injecting brine. In the first 60 min, the intensive variations occurred at a depth of 2 meters on the dam slope nearby the injection borehole WH-1. After that, the brine seepage feasibly moved downward along the interface between the weathering sandstone and sandstone. Up to 180 min, the brine flowed down into the permeable sandstone layer. After 14 h, the brine-content seepage finally stopped at the slope toe. These elapsed-time resistivity variation images also pointed out the brine seepage path in the slope mass beside the spillway. In Fig. 8, the possible flow paths of brine seepage are marked with red arrows which represent the spatial changes on resistivity variation images at different measurement moments.

The potential sliding surface usually occurs at the interface of two strata with significant differences in permeability, for example, sandstone-shale and sandstone-mudstone, or at the accumulation zones of groundwater (Richards et al., 1978; Hung, 2016). The long-term restored groundwater gradually softens the shale strength as well (Horn and Deere, 1962). Comparing the resistivity variation images in Fig. 8, Fig. 9 demonstrates that a brine seepage path passes along the bottom of the permeable sandstone layer, right above the relatively impervious layer of sandstone with mudstone at the distance of 20~37 meters. The flowing path of brine represents a wetting surface formed at the steep geological interface, marked with a bold red dashed line, around the middle part of the dam slope. Ordinarily, such a weak layer interface would possibly develop as a potential sliding surface, about 3~5 meters

deep when an extreme rain or typhoon occurs. As a contrast to the findings in the on-site investigation report (Liming, 2014), the sliding depth is highly consistent with the measured depth, i.e., 3.8 meters, of the surface sliding.
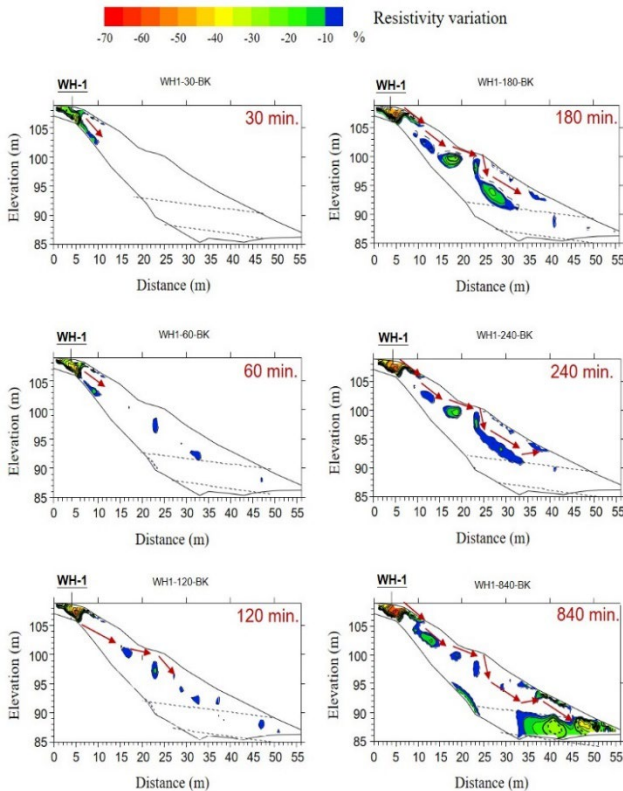
Fig. 8. Resistivity variation images of brine seepage tracing technique along investigation Line WH-1S (variation more than -10%)
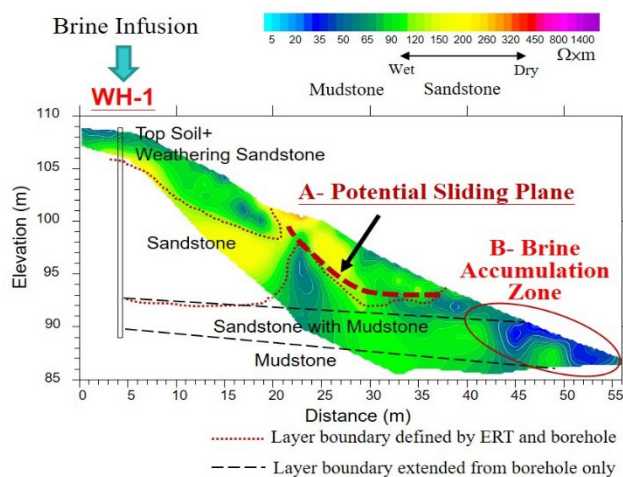

Fig. 9. Possible sliding plan and seepage accumulation zone along survey Line WH-1S

In addition, the terminal of the brine seepage will accumulate at the slope toe, labelled as an askew red oval, as shown in Fig. 9. Consequently, the seepage standing on

the slope toe could not only lead to groundwater effusion but also gradually soften the strengths of soils. Accordingly, an on-site rusty fountain at the lower slope surface verifies the existence of the groundwater flows identified on the electrical resistivity tomography-based brine tracing image. The slope surface of undermined sandstone with mudstone reveals shallow surface sliding and erosion as well.

4.3 Non-Sliding Zone Investigation

In Fig. 10(a), the geomaterials in the WH-2 borehole sampling from the ground surface are, in series, composed of mudstone, loose sandstone with mudstone, mudstone, interlayered loose sandstone/mudstone, mudstone, loose sandstone with mudstone, loose sandstone, mudstone, loose sandstone, and mudstone. The background image of electrical resistivity tomography along survey Line WH-2S, as shown in Fig. 10(b), had a good consistency with the geological findings at borehole WH-2. The black dashed lines represented the geological layer boundaries extended from the borehole sampling only. The red dotted lines represented the geological layer boundaries jointly defined by both the electrical resistivity tomography image and borehole sampling information. In the background image of electrical resistivity tomography, the mudstones usually corresponded to relatively lower resistivity zones, i.e., dark blue, blue, and green shades. The yellow, light green, and red modes, i.e., relatively higher resistivity zones, indicated the loose sandstone mixing with mudstone or interlayered loose sandstone/mudstone.
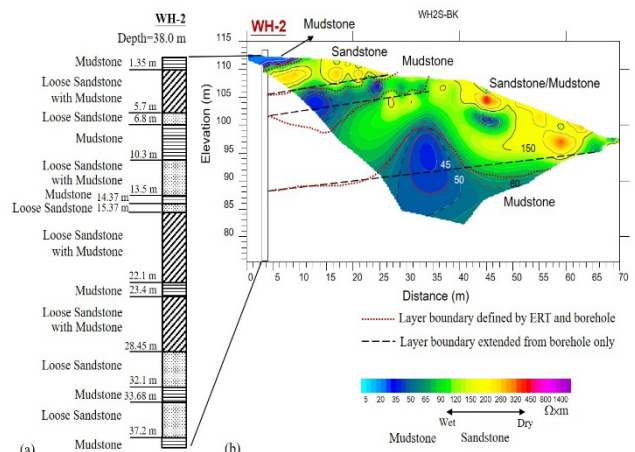

Fig. 10. (a) Geological column at WH-2; (b) background image of electrical resistivity tomography along investigation Line WH-2S (Geological profile data from Liming, 2014)

Fig. 11 represents the resistivity variation images (variation more than -10%) along survey Line WH-2S after infusing brine into the borehole WH-2. The resistivity variation images represented the changes before and after the brine injection. Moreover, brine influx could cause a significant decrease in the resistivity values in the

downstream slope of the rockfill dam. The most intensive resistivity variation zones represented the most intensive impact positions from the injected brine. Within the first 240 min, the relatively significant resistivity variations (-20% maximum) occurred at the sandstone/mudstone interlayer, around the elevations of 85~100 meters and the measurement distances of 15~30 meters. As time increased, the resistivity variation range expanded outward, but relatively limited. As brine injection stopped, the spatial expansion of resistivity variation vanished in 840 min. This phenomenon possibly revealed that the brine seepage is determined by near-borehole diffusion. Therefore, coverage on the resistivity variation depended upon continuous brine infusion. No significant seepage direction or accumulation zone developed in the elapsed-time variation images of electrical resistivity tomography. In fact, broomy bushes and grass cover the whole slope surface, and no surface erosion or sliding scars were found along survey Line WH-2S, as shown on the right side of Fig. 4.

In brief, observing brine seepage could rapidly reflect the possible groundwater or leakage flow path in specific geological layers and accumulation zones as well. Tracing the brine seepage path can also provide the information about potential sliding planes on a dam mass by using the elapsed-time electrical resistivity tomography technique in a few hours.
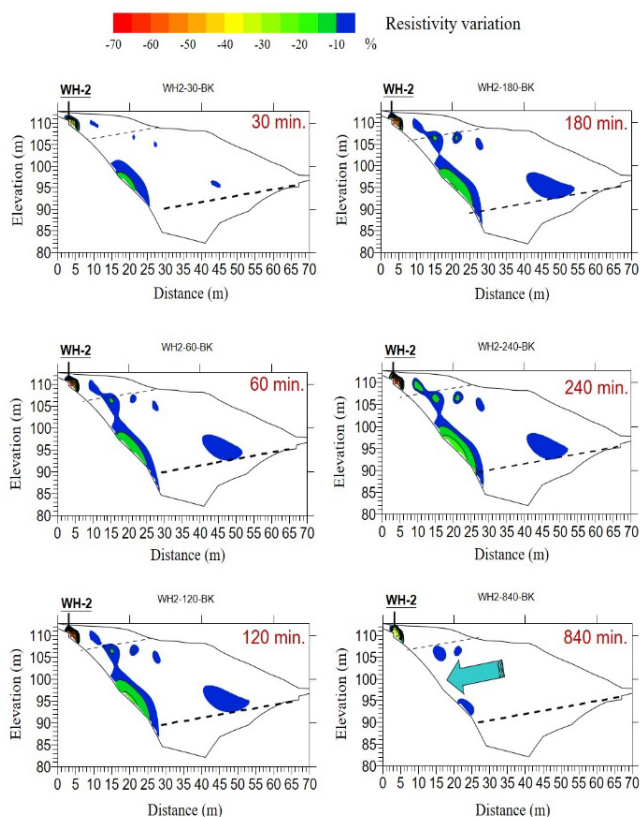
Fig. 11. Resistivity variation images of brine seepage tracing technique along investigation Line WH-2S (variation more than -10%)

5. CONCLUSION

The brine seepage tracing technique based on an electrical resistivity tomography approach was applied to investigate the potential seepage flowing through a dam mass. The conclusions can be drawn as the followings:

1. A downhole electrical resistivity tomography-based brine tracing technique plays an active role in detecting the seepage path through the dam mass continuously. Like a penetrant, the injected brine flows along the groundwater seepage path. Monitoring the elapsed-time variation images of electrical resistivity tomography can effectively identify the spatial distribution of the seepage and the primary flow direction through a dam slope in a few hours. This method will make it easier to track the groundwater seepage path than the traditional detection of electrical resistivity tomography technology.

2. The seepage path usually passes along with the bottom of a permeable sandstone layer, above the relatively impervious mudstone layer. The path of the brine flow represents a wetting surface formed at the interface between permeable and impervious geological layers. Such a geological weak plane would progressively develop as a potential sliding surface during severe rain or storm period.

3. The resistivity variation range slowly expands from the brine infusion borehole in a permeable geological layer. When no significant seepage direction or accumulation zones is observed in the elapsed-time variation images of electrical resistivity tomography, this phenomenon could indicate that the brine seepage is affected by near-borehole diffusion.

4. In the future, geotechnical or dam engineers can consider to use the brine tracing technique based on electrical resistivity tomography to effectively screen the possible spatial distributions of groundwater seepage or leakage in a dam mass and take appropriate contingent countermeasures preventing from further deterioration events.

REFERENCES

Dahlin, T. 1993. On the automation of 2D resistivity surveying for engineering and environmental applications. Ph.D. Thesis, Department of Engineering Geology, Lund University, Lund, Sweden.

Daily, W., Ramirez, A., Binley, A., LaBrecque, D. 2005. Electrical resistance tomography- Theory and practice. in Near-Surface Geophysics. Investigations in Geophysics No. 13, edited by Butler, D.W., Society of Exploration Geophysicists, Tulsa, Oklahoma, U.S.A., 525–550.

Horn, H.M., Deere, D.U. 1962. Friction characteristics of minerals. Géotechnique, 12, 318–319.

Hung, J.-J. 2016. An outline of elementary engineering geology. 5th edition, Sino-Geotechnics Research and Development Foundation, Taipei, Taiwan. (in Chinese)

Liao, J.-T., Chen, C.-W., Kao, C.-C., Hsieh, C.-H., Chen, S.-E., Kuo, C.-S., Huang, C.-Y., Tsai, W.-T., Wang, C.-W. 2019. The deep-seated landslide is a critical illness for mitigation, but is not absolutely incurable~ A case study of Woo-Wan-Chai Landslide area on the Alishan Highway. Sino-Geotechnics, 161, 7–18. (in Chinese)

Liming Engineering Consultants (Liming). 2014. Safety investigation and evaluation of the spillway and dam levee of the Renyi lake reservoir. A report to the 5th Branch of Taiwan Water Corporation, Chia-Yi, Taiwan. (in Chinese)

Lin, C.-C., Chung, C.-C., Lin, C.-P. 2019. Evaluation of engineering geophysical methods applied in characterization of large scale deep-seated landslides. Sino-Geotechnics, 161, 81–90. (in Chinese)

Loke, M.H. 2000. Electric imaging surveys for environmental and engineering studies— A practical guide for 2-D and 3-D surveys. ABEM Instrument AB, Sunbyberg, Sweden.

National Chiao Tung University (NCTU). 2005. Review of monitoring problems and non-destructive testing methods for evaluation dam performance. Report No. MOEA-WRA-0940206, Water Resources Agency, Ministry of Economic Affairs, Taichung, Taiwan. (in Chinese)

Pellerin, L. 2002. Applications of electrical and electromagnetic methods for environmental and geotechnical investigations. Surveys in Geophysics, 23, 101–132.

Richards, L.R., Leg, G.M.M., Whittle, R.A., 1978. Appraisal of stability conditions in rock slopes. in "Foundation Engineering in Difficult Ground". edited by Bell, G.B., Butterworth & Co. Ltd., London, U.K., 449–492.

Schuster, R.L., Krizek, R.J. 1978. Landslides— Analysis and control. Transportation Research Board Special Report 176, Washington, D.C., U.S.A.

Sjödahl, P. 2006. Resistivity investigation and monitoring for detection of internal erosion and anomalous seepage in embankment dams. Ph.D. Thesis, Department of Engineering Geology, Lund University, Lund, Sweden.

Society of Exploration Geophysicists of Japan. 2014. Application manual of geophysical methods to engineering and environmental problems. European Association of Geoscientists & Engineers (EAGE), Houten, the Netherlands.

Taiwan Geotechnical Society (TGS). 2011. The cause investigation report on landslide at mileage 3.1-km of freeway no.3. A Forensic Investigation Report to Ministry of Transportation and Communications, Taipei, Taiwan. (in Chinese)

Tesfaldet, Y.T., Puttiwongrak, A. 2019. Seasonal groundwater recharge characterization using time-lapse electrical resistivity tomography in the Thepkasattri Watershed on Phuket Island Thailand. Hydrology, 6, Paper 36.

Wang, H., Hu, C.-H. 2015. Identification on unknown bridge foundations using geophysical inspecting methods. The e-Journal Non-Destructive Testing, 20, 11, 905–912.

Wang, H., Hung, J.-J. 2012. Failure on a roadside dip slope with partial anchorage system. in advances in transportation geotechnics II, 180–185.

Ward, S.H. 1980. Electrical, electromagnetic, and magnetotelluric methods. Geophysics, 45, 1659–1666.

Ward, S.H. 1990. Resistivity and induced polarization methods. in Geotechnical and Environmental Geophysics, 1, 147–189.

Wightman, W.E., Jalinoos, F., Sirles, P., Hanna, K. 2003. Application of Geophysical Methods to Highway Related Problems. FHWA Report No. FHWA-IF-04-021, Central Federal Lands Highway Division, Federal Highwat Administration (FHWA), Lakewood, Colorado, U.S.A.